

# Neural Network Ensembles: Combining Multiple Models for Downscaling of Soil Moisture

Soo See Chai, Kok Luong Goh

**Abstract**— Soil moisture estimation is important for land surface modeling and climate modeling, with soil moisture being employed as a critical parameter. Although, the derivation of soil moisture from passive microwave remote sensing has been theoretically and practically proven to be possible, its spatial resolution however tends to be coarse-grained, at a range of about 20-40 km. As this does not satisfy the requirements of models using higher resolution grids, it is thus desirable to downscale soil moisture to finer resolutions of between 1 to 5 km. Neural network ensembles are known to be able to effectively improve the overgeneralization that arises from the combination of a set of neural network classifiers with a diverse range of error distributions. In this paper, a neural network ensemble method was explored to downscale soil moisture content from 20km to 2km resolution. The dataset used in this experiment was captured using low resolution L-band passive microwave observations from regional air-borne measurements in the study of Goulburn River catchment in Australia. The results have shown that by using a neural network ensemble, an average accuracy of 2.33% can be obtained for the downscaled soil moisture at a 2km resolution.

**Index Terms**— downscaling, ensemble neural network, radiometer, soil moisture.

## I. INTRODUCTION

Soil moisture estimation plays an important role in hydrological cycles and land-surface interaction. The importance of soil moisture across of variety of scientific areas has been documented in various studies. Examples of these areas include: weather forecast [1-3], rainfall-runoff transformation model [4-6], soil evaporation and plant transpiration [7-9]. Despite its importance in various areas, the conventional point measurement of this variable is difficult to achieve regular, reliable and at regional scale. Remote sensing, on the other hand, provides a potential technique to access this variable at various scales. In particular, passive microwave has been the most successful of remote sensing approaches for soil moisture estimation, due to its ability to penetrate cloud, its direct relationship between soil moisture through soil's dielectric constant, and a reduced sensitivity to land surface roughness and vegetation cover [10].

Artificial neural networks (ANN) have been widely used in water resources and hydrology applications as they are robust to noisy data and have been suited for approximating multivariate non-linear relations among variables.

The Neural network ensemble method is a meta-learning paradigm where multiple neural networks are jointly used to solve a problem [11]. In the earlier work, the authors had

used Backpropagation Neural Network for soil moisture retrieval [10, 12, 13] and for downscaling of soil moisture [14]. In this paper, the neural network ensemble method is used to downscale soil moisture from 20km to 2km from the low resolution L-band passive microwave observations.

## II. DATA

The study area of NAFE'05 is the Goulburn River catchment, a sub-humid to temperate area located in south-eastern Australia, approximately 300km north-west of the city of Sydney [15]. This catchment has two intensively monitored sub-catchments, the Krui River (562 km<sup>2</sup>) and Merriwa River (651 km<sup>2</sup>) in the northern half of the catchment.

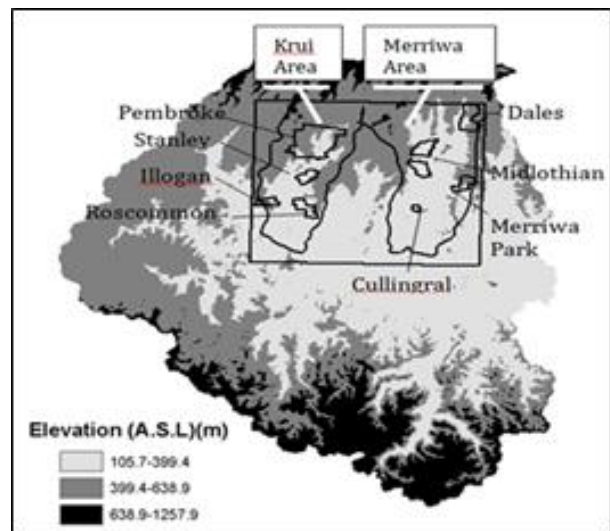


Figure 1. Overview of NAFE'05 focus farms within Krui and Merriwa areas

### A. Regional Airborne Data

Regional airborne measurements had been made using a two-seater motor glider equipped with the Polarimetric L-band Multibeam Radiometer (PLMR) which allows very high resolution passive microwave (~50 m) observations to be made at 1 km nominal resolution over the entire study area on November 7<sup>th</sup>, 14<sup>th</sup> and 21<sup>st</sup> 2005. The radiometer was flown in 'pushbroom' configuration, yielding six across track observations from each aircraft location: brightness temperature (T<sub>b</sub>) at H- and V-polarization at incidence angles ±7°, ±21.5° and ±38.5°. The beamwidth is 17° resulting in an overall 90° field of view.

Manuscript received December, 2013.

Soo See Chai, Department of Software Engineering and Computing, Faculty of Computer Science and Information Technology, University of Sarawak Malaysia.

Kok Luong Goh, International College of Advanced Technology Sarawak.

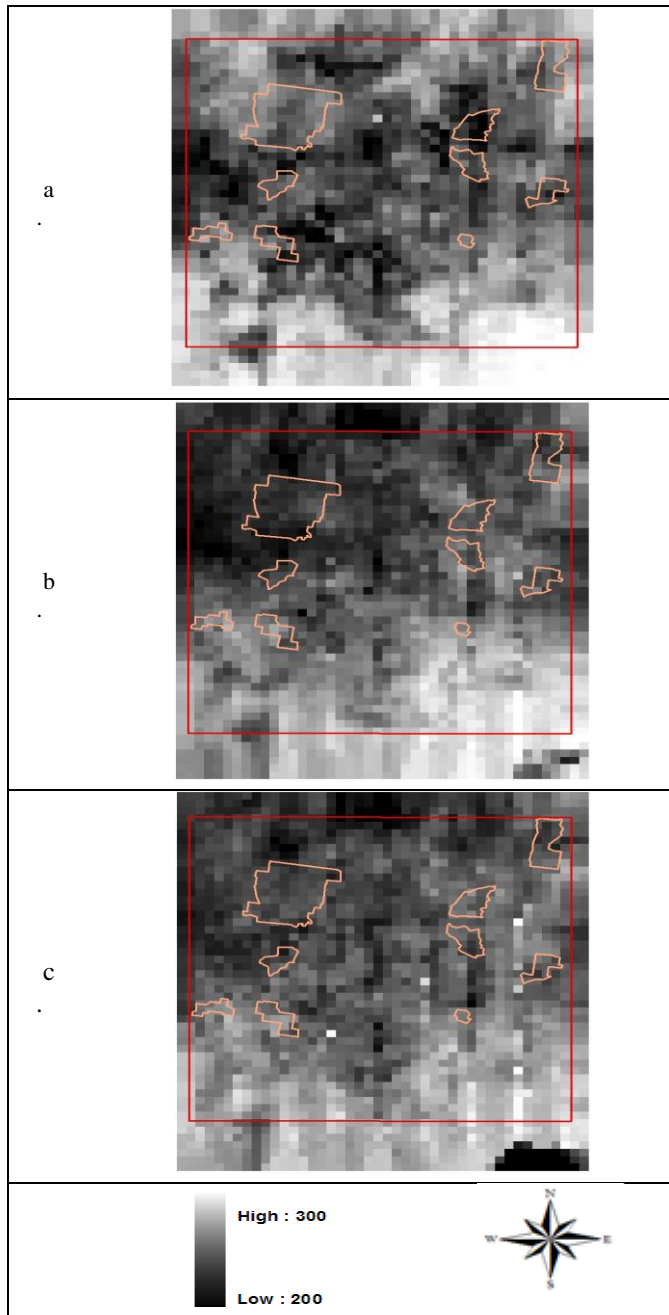


**Figure 2. Normalized H-polarized brightness temperature for (a) November 7th, (b) November 14th, and (c) November 21st at 1 km resolution. The boundaries for the focus farms are shown in beige while the boundary for the study area is shown in red.**

A full pixel overlap between adjacent flight lines was guaranteed in order to avoid data gaps and ensure full coverage of the entire area. The PLMR data used in this study was georeferenced at H- and V-polarizations and calibrated internally against cold and warm loads [16].

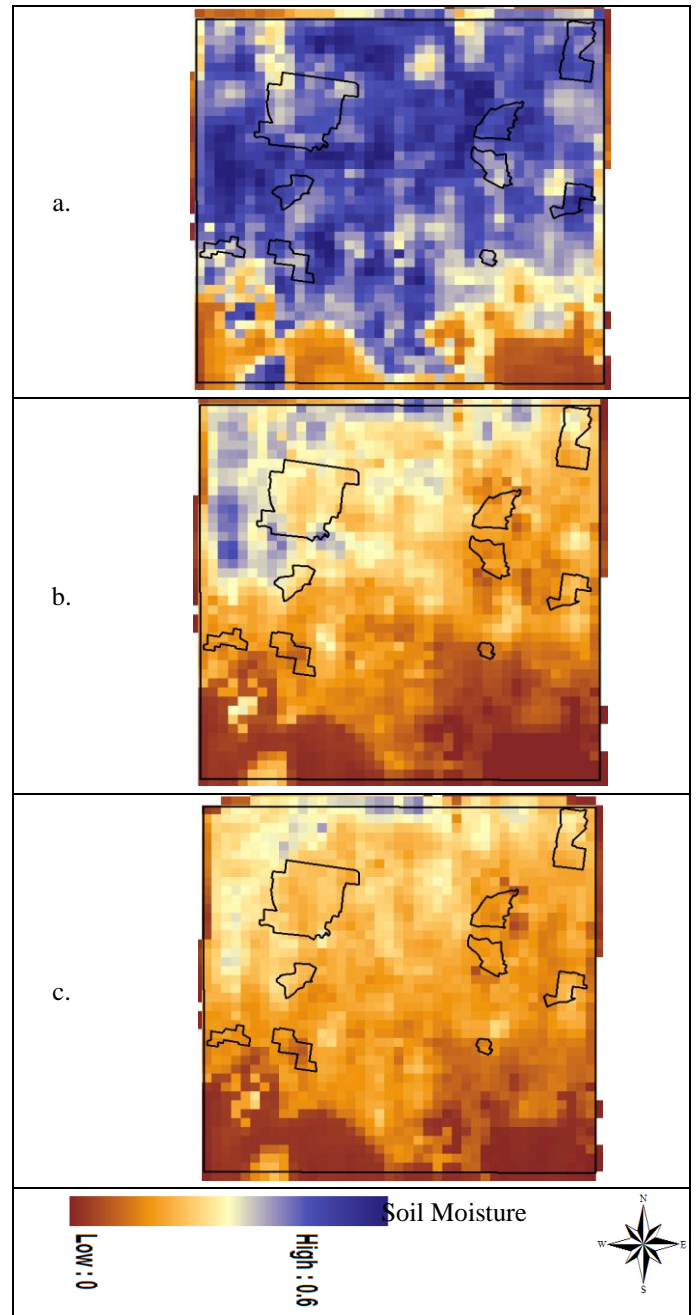


**Figure 3. L-MED retrieved soil moisture from regional airborne observations (1km) on a. 7th Nov, b. 14th Nov and c. 21st Nov 2005. The boundaries of the focus farms and the whole study area are shown in solid lines.**

To normalize the data to  $\pm 38.5^\circ$ : The daily average over land target is first computed for each beam. Next, a correction factor is then computed by taking the ratio between the averages of each beam to the average of the reference beam. All the data for each beam on each day are then corrected using this correction factor as in:

$$Tb_i^N = Tb_i \times \left( \frac{\overline{Tb_i}}{\overline{Tb_{ref}}} \right) \quad (1)$$

where  $Tb_i$  is the individual  $Tb$  acquisition to be normalized,  $Tb_i^N$  is the normalized value,  $\overline{Tb_i}$  and  $\overline{Tb_{ref}}$  are the daily average  $Tb$  of the beam to be normalized and the beam taken as reference

respectively. The normalized  $Tb$  is gridded into a reference grid with uniform resolution. With averaging several individual  $Tb$  acquisitions into one  $Tb$  value for each cell, anomalies in individual readings are eliminated and the signal noise is reduced. Figure 2 shows the aggregated normalized brightness temperature for H-polarized data on Nov 7th, 14th and 21st.

### B. 1-km Soil Moisture Data

The 1 km soil moisture product was produced and validated using L-MEB (L-band Microwave Emission of the Biosphere) model applying the brightness temperature observations made with the PLMR radiometer (at incidence angle of  $\pm 38.5^\circ$ ) across the NAFE'05 study area. The soil moisture maps derived from the 1 km airborne data have two major advantages with respect to ground point measurements which make them desirable for the objective of ground-truthing coarse-scale soil moisture retrieval: (i) they have larger extent, covering the entire study area and therefore characterize the soil moisture variability within all the coarse-scale pixel, and (ii) each soil moisture observation represents an integrated value over a 1km area, therefore overcoming the limitation of point data which only provide information for the domain sensed by ground probe (a few centimeters) at specific location. The retrieved soil moisture shows interesting spatio-temporal dynamics which reflects the rainfall regime experienced by the area during the field experiment. Wet condition on November 7th was due to the heavy rain heavy rainstorms that showered the study area at the beginning of the experiment (20mm over October 30th and 31st), followed by more intense rainfall on November 5th (21mm). The period between November 5th and 23rd was characterized by little or no rainfall and accordingly drier soil moisture conditions were retrieved for November 14th and 21<sup>st</sup>.

### C. MODIS Data

The MODIS data used in the downscaling algorithms are composed of MODIS/Aqua Surface Reflectance Daily L2G Global 250 m and MODIS/Aqua Land Surface Temperature and Emissivity Daily L3 Global 1 km products. The MODIS NDVI (Normal Difference Vegetation Index) was calculated using Band 1 and Band 2 of the MODIS/Aqua Surface Reflectance L2G Global 250 m product. The MODIS/Aqua data were selected since there is no significant discrepancies between the NDVI values derived from Terra and Aqua satellites of MODIS [17] and all the data during the regional observations were available from this satellite image.

## III. ALGORITHM DESCRIPTION

In this paper, the method proposed by [18] is utilized using the ANN model with modification. According to [18], the relationship between the downscaled soil moisture  $\theta$ , and the SMOS scaled soil moisture,  $\theta_{SMOS}$  is a linear relationship:

$$\theta = \theta_{SMOS} + \theta_C SMP_{MODIS} \quad (2)$$

where,  $\theta_C$  : characteristic volume fraction, and

$$SMP_{MODIS} = \frac{\Delta\beta_{MODIS}}{1 - \beta_{MODIS}} \quad (3)$$

with,

$\beta_{MODIS}$  : MODIS-derived soil evaporative efficiency, and  $\Delta\beta_{MODIS}$  : difference between MODIS-derived soil evaporative efficiency and its integrated value at the SMOS scale ( $\int d\beta/d\theta d\theta$ ).

$\beta_{MODIS}$  can be written as:

$$\beta_{MODIS} = \frac{T_{max} - T_{MODIS}}{T_{max} - T_{min}} \quad (4)$$

where,

$T_{max}$  : soil temperature at minimum soil moisture

$T_{min}$  : soil temperature at maximum soil moisture

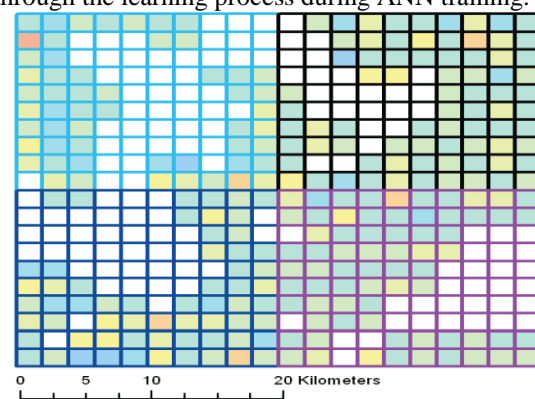
$T_{MODIS}$  : soil skin temperature derived from MODIS data at the time of interest

By assuming that  $T_{max}$  and  $T_{min}$  are mostly uniform within the SMOS pixel and the integral  $\int dT/d\theta d\theta$  is approximately equal to the areal average of  $T_{MODIS}$  (designated as  $T_{SMOS}$ ), can be computed as:

$$SMP_{MODIS} = \frac{T_{SMOS} - T_{MODIS}}{T_{MODIS} - T_{min}} \quad (5)$$

In order for the ANN to learn the downscaling relationship in equation (5), the ANN considers the following three values as input:  $\theta_{SMOS}$ ,  $\theta_C$  and  $SMP_{MODIS}$  in order to map the desired soil moisture  $\theta$ . The value of  $\theta_{SMOS}$  is obtained by aggregating the soil moisture value at the desired resolution from the 1 km L-band derived soil moisture values and the values of  $SMP_{MODIS}$  are then calculated from the MODIS.

The  $T_{surf,MODIS}$ ,  $T_{SMOS}$ ,  $T_{max}$  and  $T_{min}$  values are estimated from the MODIS/Aqua Land Surface Temperature and Emissivity Daily L3 Global 1 km data while the  $NDVI_{min}$  and  $NDVI_{max}$  are derived from Band 1 and Band 2 of MODIS/Aqua Surface Reflectance Daily L2G Global 250m. The value of  $\theta_C$  is dependent on the value of wind speed, a value unavailable spatially for NAFE'05 data used for this study. In this study, ANN is used to learn the relationship between  $\theta$ ,  $\theta_{SMOS}$  and  $SMP_{MODIS}$  without taking into consideration the value of  $\theta_C$  and produces a functional relationship map between these three variables through the learning process during ANN training.



a. 14 Nov 2005

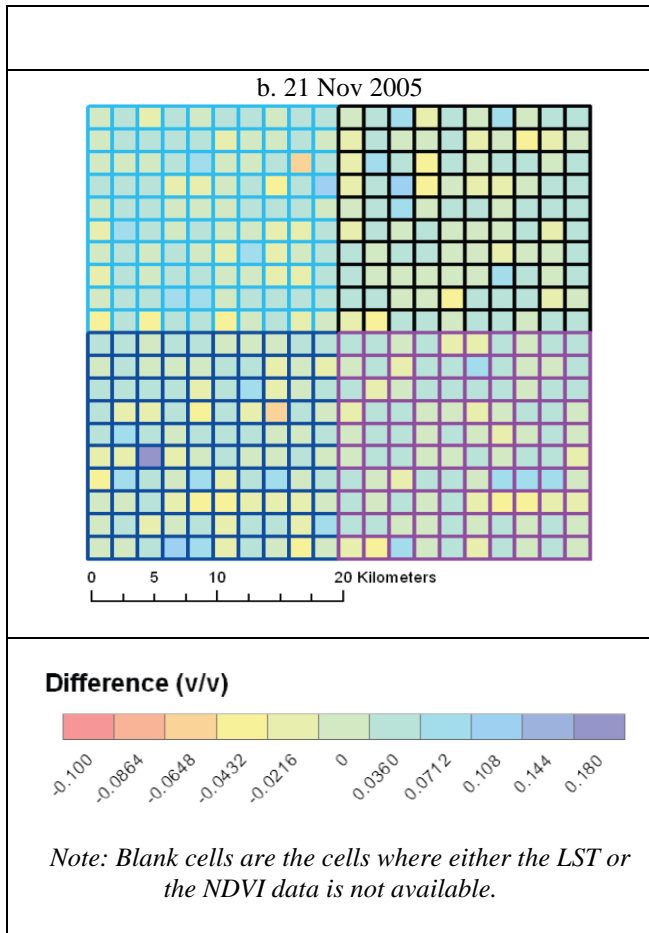


**Figure 4. Difference between the actual and predicted soil moisture for the two dates used for testing the trained ensemble neural network.**

The proposed ensemble neural networks model consists of a number of back-propagation neural network models that are trained using the same data from one single date to downscale the soil moisture from 20km to 2km resolution. Each neural network unit will focus on downscaling a particular area of 2km x2km area on the 20km resolution map area. Among the three days of when the data were taken, a single day was used for training the neural network models. The trained neural network models is used to downscale the soil moisture for the other two days. The ensemble neural network is constructed in two steps:

**i. Design the individual neural networks.**

This is done by training the neural networks on different training sets to generate a group of networks which are error uncorrelated directly. In order to obtain the different training sets, 11 sub-grid of 20kmx20km were used. To develop a particular neural network model, a sub-section of 2 x 2 pixels for data on 7<sup>th</sup> Nov 2005 for each sub-grid were used to train the network. The neural network with lowest RMSE was used to estimate soil moisture for each pixel in the 2 x 2 pixels on 14<sup>th</sup> and 21<sup>st</sup> Nov 2005.

**ii. Combining the output.**

Each of the ANN models was used to focus on predicting soil moisture at a particular location within the 20 x 20 km region. The results of these ANN models were combined by simple averaging the RMSE obtained from all ANN models for the whole 20 x 20 km region.

**IV. RESULTS**

The trained ensemble neural network were tested on two new dates. For the first date, the average Root Mean Square (RMSE) error was 2.41% v/v for date 1 (14 Nov 2005) and for the second date (21 Nov 2005), it was 2.24% v/v. From Figure 4, it can be seen the neural network ensemble model managed to predict the soil moisture accurately at a fine-grained resolution of 2km in downscaling from 20km to 2km. A strong correlation of around 0.9 was obtained for both dates (Figure 5). As some of the LST and NDVI which were used as the input for the neural network ensemble were missing, some of the soil moisture values for the cells within the 20km sub-grid could not thus be predicted. The encouraging results have shown that neural network ensembles could be used for effectively generating data driven model for downscaling of soil moisture data from 20km to 2km. Moreover the results have also shown that, in the consolidation of data from multiple neural network models has enabled the assimilation of spatial heterogeneity characteristics from the models.

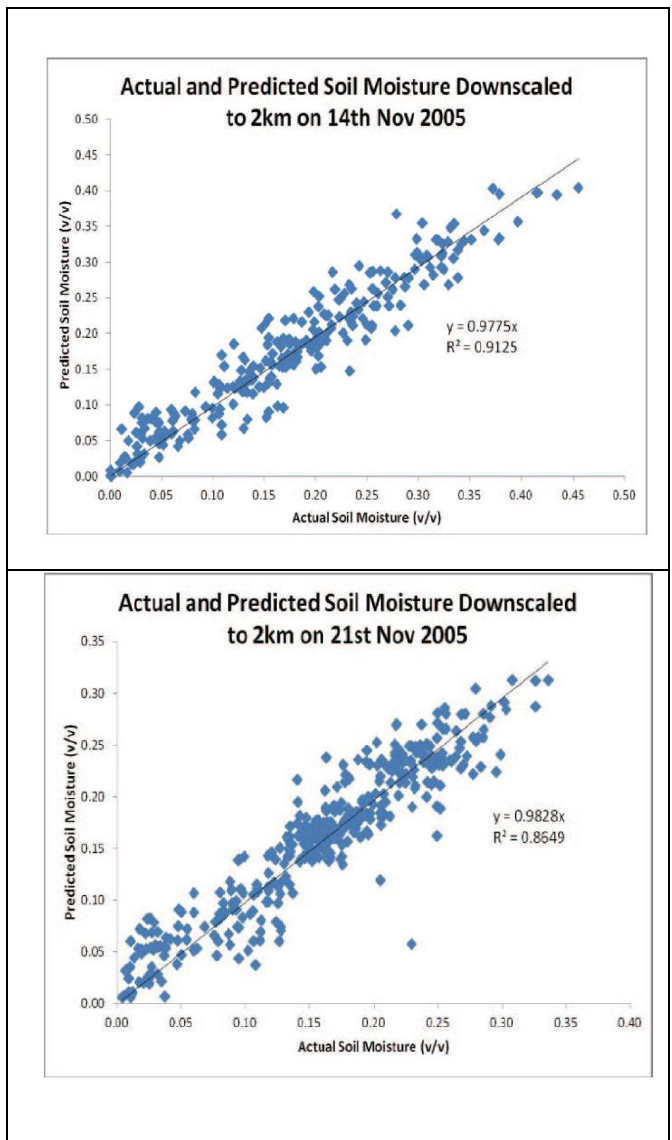


**Figure 5. Correlation between actual and predicted soil moisture downscaled from 20km to 2km for the two testing dates.**



## V. CONCLUSION

Separately trained neural networks were combined to form a single unified prediction of soil moisture aggregation and the results of the experiments have been very encouraging. The ability of the neural network ensemble method in producing results that does not fluctuate much for predicting the downscaled soil moisture at two different dates has been extremely promising. However, the practicality of such a method in real-life situation needs to be further verified using the SMOS data which was launched in November 2009.

## REFERENCES

1. de Rosnay, P., M. Drusch, J.P. Wigneron, T. Holmes, G. Balsamo, A. Boone, C. Rudiger, J.C. Calvet, and Y. Kerr. Soil Moisture Remote Sensing for Numerical Weather Prediction: L-Band and C-Band Emission Modeling Over Land Surfaces, the Community Microwave Emission Model (CMEM). in IEEE International Geoscience and Remote Sensing Symposium, 2008. IGARSS 2008. . 2008: IEEE.
2. Drusch, M., Initializing numerical weather prediction models with satellite-derived surface soil moisture: Data assimilation experiments with ECMWF's Integrated Forecast System and the TMI soil moisture data set. *Journal of Geophysical Research: Atmospheres* (1984-2012), 2007. 112(D3).
3. Rhodin, A., F. Kucharski, U. Callies, D.P. Eppel, and W. Wergen, Variational analysis of effective soil moisture from level atmospheric parameters: Application to a short-range weather forecast model. *Quarterly Journal of the Royal Meteorological Society*, 1999. 125(559): p. 2427-2448.
4. Aubert, D., C. Loumagne, and L. Oudin, Sequential assimilation of soil moisture and streamflow data in a conceptual rainfall-runoff model. *Journal of Hydrology*, 2003. 280(1): p. 145-161.
5. Crow, W.T., R. Bindlish, and T.J. Jackson, The added value of spaceborne passive microwave soil moisture retrievals for forecasting rainfall-runoff partitioning. *Geophysical Research Letters*, 2005. 32(18): p. L18401.
6. Scipal, K., C. Scheffler, and W. Wagner, Soil moisture-runoff relation at the catchment scale as observed with coarse resolution microwave remote sensing. *Hydrology and Earth System Sciences Discussions*, 2005. 2(2): p. 417-448.
7. Cavanaugh, M.L., S.A. Kurc, and R.L. Scott, Evapotranspiration partitioning in semiarid shrubland ecosystems: a site evaluation of soil moisture control on transpiration. *Ecology*, 4(5): p. 671-681.
8. Oren, R. and D.E. Pataki, Transpiration in response to variation in microclimate and soil moisture in southeastern deciduous forests. *Oecologia*, 2001. 127(4): p. 549-559.
9. Zhang, Y., C. Li, C.C. Trettin, H. Li, and G. Sun, An integrated model of soil, hydrology, and vegetation for carbon dynamics in wetland ecosystems. *Global Biogeochemical Cycles*, 2002. 16(4): p. 9-1-9-17.
10. Chai, S.-S., J.P. Walker, O. Makarynskyy, M. Kuhn, B. Veenendaal, and G. West, Use of soil moisture variability in artificial neural network retrieval of soil moisture. *Remote Sensing*, 2009. 2(1): p. 166-190.
11. Zhou, Z.-H., J. Wu, and W. Tang, Ensembling neural networks: many could be better than all. *Artificial intelligence*, 2002. 137(1): p. 239-263.
12. Chai, S.S., An Artificial Neural Network Approach for Soil Moisture Retrieval Using Passive Microwave Data: Curtin University of Technology.
13. Chai, S.-S., B. Veenendaal, G. West, and J.P. Walker. Explicit inverse of soil moisture retrieval with an artificial neural network using passive microwave remote sensing data. in IEEE International Geoscience and Remote Sensing Symposium, 2008. IGARSS 2008. . 2008: IEEE.
14. Chai, S., J.P. Walker, B. Veenendaal, and G. West, An artificial neural network model for downscaling of passive microwave soil moisture.
15. Walker, J.P. and R. Panciera, National Airborne Field Experiment 2005: Experiment Plan. Department of Civil and Environmental Engineering, The University of Melbourne, 2005.
16. Panciera, R., J.P. Walker, O. Merlin, J.D. Kalma, and E. Kim. Scaling Properties of L-band Passive Microwave Soil Moisture: From SMOS to Paddock Scale. in 30th Hydrology and Water Resources Symposium. 2006. the Institute of Engineers Australia, Launceston, Australia.
17. Jing, W., G. Ni, W. Xiaoping, and Y. Jia. Comparisons of normalized difference vegetation index from MODIS Terra and Aqua data in northwestern China. in IEEE International Geoscience and Remote Sensing Symposium, 2007. IGARSS 2007. 2007.
18. Merlin, O., J.P. Walker, A. Chehbouni, and Y. Kerr, Towards deterministic downscaling of SMOS soil moisture using MODIS derived soil evaporative efficiency. *Remote Sensing of Environment*, 2008. 112(10): p. 3935-3946.